Cosmic Ray Mass Composition by the Data of Tunka EAS Cherenkov Arrays

N. M. Budnev[2], O. A. Chvalaiev[2], O. A. Gress[2], N. N. Kalmykov[1], E. E. Korosteleva[1], V. A. Kozhin[1], L. A. Kuzmichev[1], B. K. Lubsandorzhiev[3], R. R. Mirgazov[2], G. Navarra[4], M. I. Panasyuk[1], L. V. Pan'kov[2], V. V. Prosin[1], V. S. Ptuskin[5], Yu. A. Semeney[2], B. A. Shaibonov (junior) [3], A. V. Skurikhin[1], C. Spiering[6], R. Wischnewski[6], I. V. Yashin[1], A. V. Zablotsky[1], A. V. Zagorodnikov[2]

Abstract—**The final analysis of EAS maximum (X_{max}) depth distribution derived from the data of Tunka-25 EAS Cerenkov array is presented. The perspectives of X_{max} study with the new Cherenkov light array Tunka-133 of 1 km^2 area are discussed. During the winter 2007 – 2008 the new array operated with 4 clusters of 7 detectors in each one. The analysis of experimental data has shown the unique possibilities of the new array provided by the registration of pulse waveform from each detector.**

1. Introduction

The elaborate study of primary mass composition in the energy range 10^{15} – 10^{18} eV is of crucial importance for the understanding of the origin and propagation of cosmic rays in the Galaxy. The change from light to heavier composition with growing energy marks the energy limit of cosmic ray acceleration in galactic sources (SN remnants). An opposite change from heavy to light composition at higher energy would testify the transition from galactic to extragalactic cosmic rays. Both changes are expected in the energy range under our study.

To study the mean composition we use the relation between the logarithm of mass (lnA) and the depth (X_{max}) of the extensive air shower (EAS) maximum: $<X_{max}> \sim <\ln A>$ - which is well-known from electromagnetic cascade theory. In the Tunka-25 experiment X_{max} was derived for every event from the steepness of the Cherenkov light flux lateral distribution function (LDF), resulting in an X_{max} distribution. There are two methods of estimation of the mean composition using this distribution. The first of them is a linear interpolation of <lnA> between that for protons and iron using the experimental $<X_{max}>$. The second, more correct one presented below is the statistical analysis of the total distribution. It shows the existence of a methodical distortion of estimated <lnA> for the first method.

Both methods show the beginning of composition change from light to heavy at energies above 10^{16} eV. To study the further behavior of <lnA> one needs more statistics and consequently an array of larger sensitive area and solid angle. Such an array, Tunka-133, is now under construction close to its predecessor Tunka-25. Last winter the first part of the new array operated for about 270 h during clean moonless nights. The first results and perspectives of the new array are presented below.

2. Mass composition analysis using X_{max} distribution

The detailed description of the Tunka-25 experiment and the procedure of X_{max} deriving from the LDF steepness is given in [1].

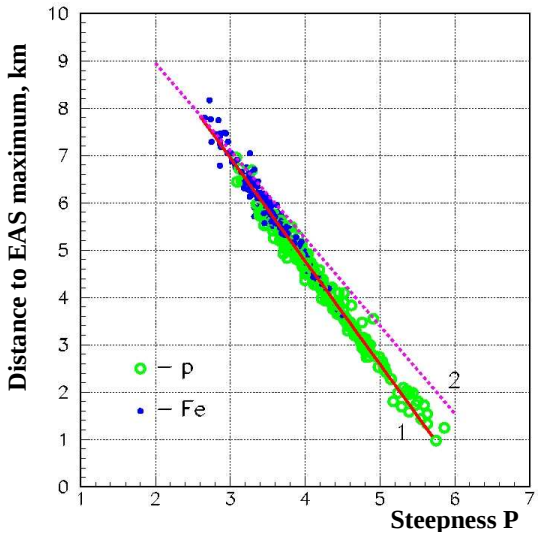

Figure 1. Simulated correlation between Cherenkov light LDF steepness and the distance of the EAS maximum.

1 – Skobeltsyn Institute of Nuclear Physics of Moscow State University, Moscow, Russia;
2 – Institute of Applied Physics of Irkutsk State University, Irkutsk, Russia;
3 – Institute for Nuclear Research of Russian Academy of Sciences, Moscow, Russia;
4 – Dipartimento di Fisica Generale Universita' di Torino and INFN, Torino, Italy;
5 – IZMIRAN, Troitsk, Moscow Region, Russia;
6 – DESY, Zeuthen, Germany.
Presenter: V.V. Prosin (tel.: +7-495-939-10-72; fax: +7-495-939-35-53; e-mail: v-prosin@yandex.ru).

The simulated connection of the LDF steepness P with the linear distance to shower maximum H_{max} is shown in fig. 1. We have to pay attention once more to the fact that all the simulated points for different primaries, different energy and different zenith angles cluster along the same straight line in fig. 1. So this correlation can be really used for measuring the EAS maximum position, taking into account the barometric formulae connecting H_{max} with X_{max}. The simulation was made for the Tunka valley level (675 m a. s. l.). A similar simulation for the EAS-TOP level (2000 m a. s. l.) shows a slight difference from the first line at large depth only.

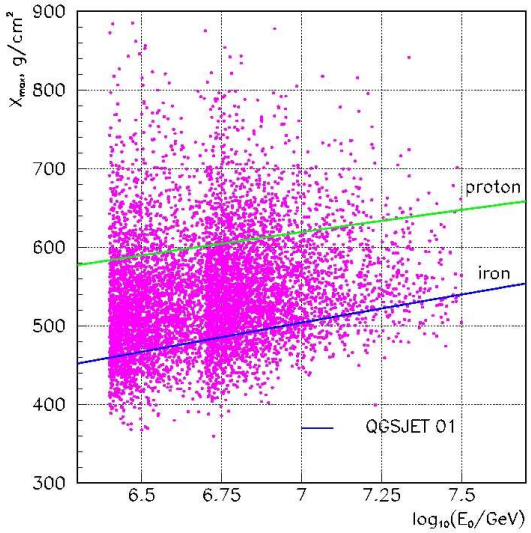

Figure 2. Depth of maximum, X_{max}, vs. primary energy E_0.

The experimental plot of the depth of the shower maximum thus obtained vs. primary energy E_0 is shown in fig. 2. It contains 7632 points. Analysis of possible distortions of the distribution has shown that there are no systematic errors for EAS with energy $E_0 > 2.5 \cdot 10^{15}$ eV and zenith angles $\theta \leq 12°$ and for $E_0 > 5 \cdot 10^{15}$ eV and $\theta \leq 25°$. The distributions inside narrow logarithmic energy bins (0.1) have been analyzed. The analysis was done as follows. The experimental X_{max} distribution is compared with the simulated one. The simulated distribution is constructed from 4 partial distributions for different nuclei groups – p, He, CNO and Fe. Partial distributions are simulated with a "model of experiment" code assuming the QGSJET-01 model of primary interaction. The code itself includes all the essential parameter correlations and distributions extracted from CORSIKA and takes into account all the apparatus errors and selection of events. A detailed description of this code is given in [1]. The weight of each group is selected for the best fit of the experimental distribution. The result for one of the logarithmic bins ($6.4 < \log_{10}(E_0/GeV) < 6.5$) is shown in fig. 3. We note that QGSJET-01 provides the best fit of the left edge of the distribution when compared with the other models.

In principle the result of this procedure can give the relative weight of each group of nuclei within the total composition. But limited statistics and the relatively large width of the partial distribution make it almost impossible to distinguish between proton/helium and CNO/iron groups.

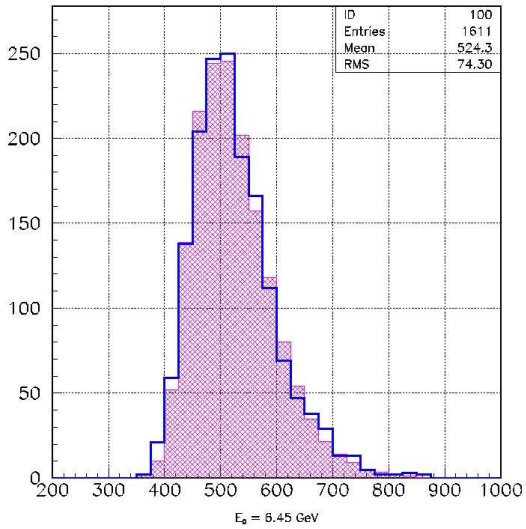

Figure 3. Distribution of the depth of the EAS maximum for $6.4 < \log10(E_0/GeV) < 6.5$. Line – experiment, filled area – simulation for 70% of light (p+He) and 30% of heavy (CNO+iron) nuclei.

A more stable estimation can be made for the percentage of light (p+He) and heavy (CNO+iron) nuclei in the primary composition. And the most stable is the estimation of the mean logarithmic mass <lnA>. The experimental dependence of <lnA> on primary energy E_0 is shown in fig. 4.

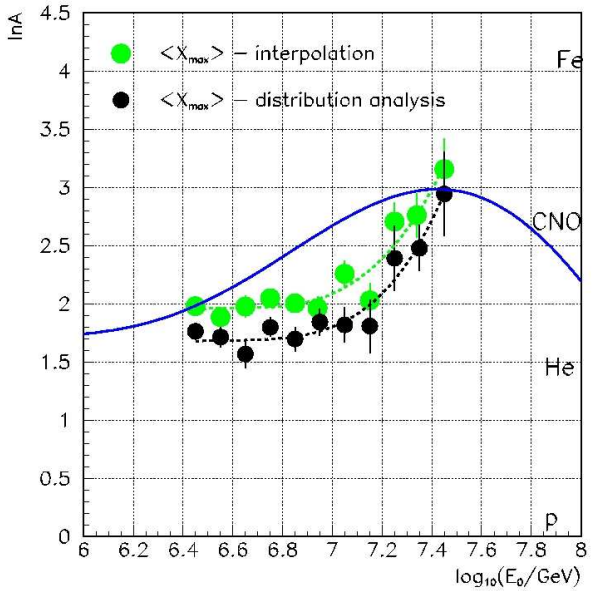

Figure 4. Mean logarithmic mass vs. primary energy E_0. Dense curve is the theory [2], dotted curves are the smoothing approximations of the experimental points.

The theoretical curve in fig. 4 is a simulation from [2]. One sees that the old method of interpolation shifts <lnA> systematically by about 0.25 towards heavier composition, compared to the more strict method of the analysis of the full distribution. The mean value obtained with the second method for the knee range of energies ($3 \cdot 10^{15}$ eV) coincides with that obtained in the recent balloon experiments for energy about 10 TeV [3]. The rise of <lnA> for energies above 10^{16} eV is well visible.

3. TUNKA-133 ARRAY

To study the mass composition behavior at the intermediate energy range $10^{16} - 10^{18}$ eV, the new array Tunka-133 is under construction [4].

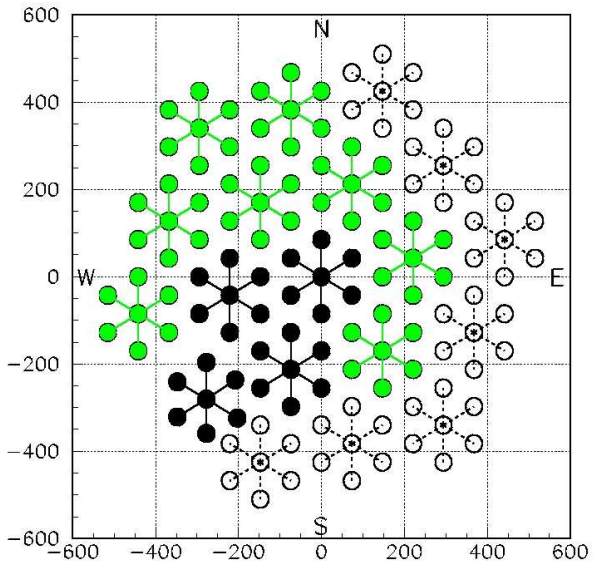

Figure 5. Plan of the Tunka-133 array. Black – 4 clusters operated in winter 2007-2008, grey – 8 clusters ready for operation in winter 2008-2009, open circles – the last 7 clusters to be deployed in 2009.

The array will consist of 133 detectors grouped into 19 clusters each composed of 7 detectors. The map of the array is shown in fig. 5. The new array provides much more information than the previous one. Each detector signal is digitized by a FADC with time step 5 ns. So the waveform of every pulse is recorded, together with the preceding noise, as a total record of 5 μs duration. The minimal pulse FWHM is about 20 ns and the dynamic range of amplitude measurement about 10^4. The latter is achieved by two channels for each detector taking signals from anode and intermediate dynode of the PMT with different additional amplification factors.

Four clusters marked with black color in fig. 2 operated last winter between November and April. Data have been recorded over 270 hours during clean moonless nights. The average trigger rate was about 0.3 Hz, the number of the registered events was about 300000.

4. RECONSTRUCTION OF EAS PARAMETERS

A. Structure of the codes for data processing.

The program of calibration and reconstruction of EAS parameters consists of three main blocks of codes.

1. The first block works with the primary data recorded separately for each cluster and includes the following steps. The analysis of 5 μs record with a measurement step 5 ns; a pulse search defined by a noticeable increase of the absolute amplitude value over 5 or more consecutive points; the definition of a zero level as a mean amplitude during the first 1500 ns of the record; a correction of the measured amplitudes by subtraction of the zero level; fitting of the modified amplitudes with a four-parameter function [5]; definition with this function of three key parameters of the pulse: front delay at a level 0.25 of the maximum amplitude (t_i), pulse area (Q_i) and full width on half-maximum $FWHM_i$.

2. The second block of codes works with files of pulse parameters. This block unites the data of different clusters and provides the time and amplitude calibration. Data from various clusters are merged to one event, if the time difference for cluster triggers is less than 2 μs.

The time calibration consists of the shower flat front reconstruction by the measured delays t_i, separately for each cluster. The distributions of the delays with respect to the reconstructed front are analyzed for each detector and each inherent delay (defined basically by the communication cable length) is corrected. The procedure is repeated until the residual is less than 1 ns. The final EAS arrival direction is defined by data of the cluster with the maximum amplitudes. The amplitude calibration is provided in the same way described in our previous work [1].

3. The third block of programs reconstructs the EAS core location, the primary energy and the depth of the shower maximum.

B. EAS core reconstruction by the density of Cherenkov light flux Q_i.

The first method of EAS core location reconstruction is fitting the Q_i by the lateral distribution function (LDF) with varied parameters of steepness (P) and light density at a core distance 175 m (Q_{175}). This function was first suggested by the members of our collaboration in [6], and it is changed here to include large distances to a treatment:

$$\begin{aligned} Q(R) &= Q_{kn} \cdot \exp((R_{kn}-R)\cdot(1+3/(R+3))/R_0), \quad R < R_{kn} \\ Q(R) &= Q_{kn} \cdot (R_{kn}/R)^{2.2}, \qquad\qquad R_{kn} < R < 200 \text{ m} \\ Q(R) &= Q_{kn} \cdot (R_{kn}/200)^{2.2} \cdot ((R/200+1)/2)^{-b}, \quad R > 200 \text{ m} \end{aligned} \tag{1}$$

Here R is the core distance (in meters), R_0 is a parameter of the first branch of LDF, R_{kn} is the distance of the first change of LDF, Q_{kn} is the light flux at the distance R_{kn}. The second change is at the core distance 200 m, b is the parameter of the third branch. This branch is checked till the distance 700 m

with CORSIKA simulated events.

These 4 variables are strictly connected with two main parameters of the LDF – density at 175 m Q_{175} and steepness P:

$$
\begin{aligned}
&Q_{kn} = Q_{175}\cdot(R_{kn}/175)^{-2.2} \\
&R_0 = \exp(6.79 - 0.564\cdot P), \text{ (m)} \\
&R_{kn} = 207 - 24.5\cdot P, \text{ (m)} \\
&b = 4.84 - 1.23\cdot\ln(6.5-P), \quad P < 6 \\
&b = 3.43, \qquad P > 6
\end{aligned}
\tag{2}
$$

C. EAS core reconstruction with measured widths of Cherenkov light pulses $FWHM_i$.

In addition to the traditional method above described a new method of EAS core reconstruction using Cherenkov light pulse FWHM has been designed and included into the code. To fit the experimental FWHM, the empirical width-distance function (WDF) is used. It has a very simple analytic form for FWHM>20 ns:

$$\mathrm{FWHM}(R) = 11\cdot(\mathrm{FWHM}(400)/11)^{(R+100)/500}, \text{ (ns)} \tag{3}$$

This expression approximates the result shown below for core distances R<500 m. To get the WDF for higher distances and to connect FWHM(400) with the shower maximum depth we plan additional CORSIKA simulations.

The EAS maximum depth X_{max} will be reconstructed for each event by two independent methods from LDF steepness P and the parameter FWHM(400).

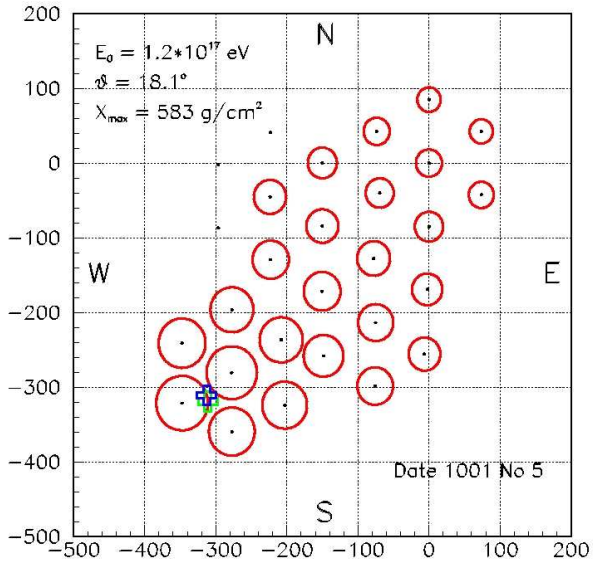

Figure 6. An example of an experimental event. The radii of the circles are proportional to the logarithm of the Cherenkov light flux.

An example of a reconstructed shower is presented in fig. 6. The LDF and WDF for this event are shown in fig. 7 and 8, respectively.

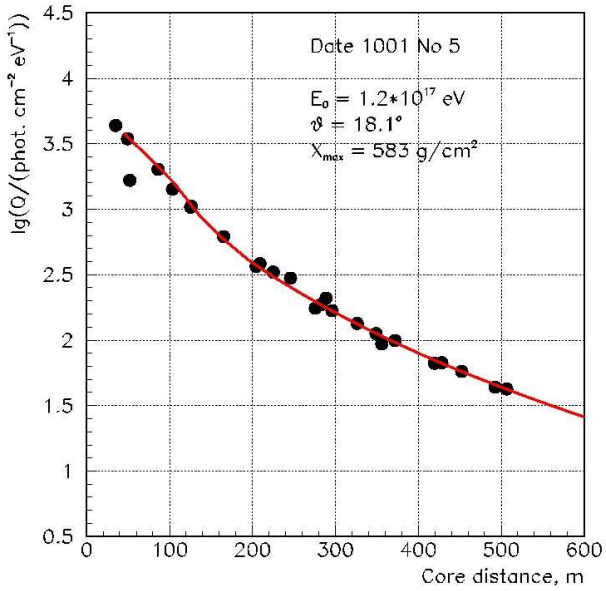

Figure 7. Lateral distribution resulting from fitting the measured light fluxes (points) with the expression (1) (curve) for the event from fig. 6.

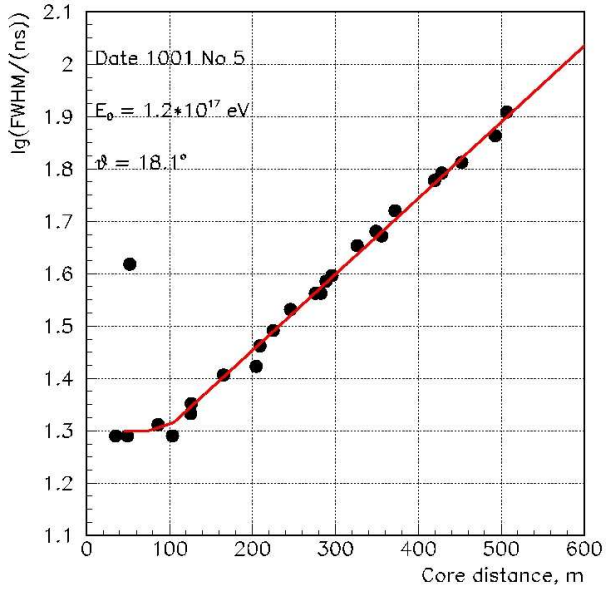

Figure 8. Dependence of Cherenkov light pulse width on the core distance for the event from fig. 6. Points – experiment, line – approximation by expression (2).

5. PERSPECTIVES OF THE NEW METHOD OF EAS PARAMETERS RECONSTRUCTION WITH PULSE DURATIONS

The good agreement of the experimental pulse durations with WDF (2), the absence of FWHM random fluctuations and a more simple expression for WDF than for LDF seems to

allow us applying the new method of EAS core reconstruction not only inside the array geometry, but also outside up to a certain distance.

A similar idea of reconstruction of EAS core distance using pulse width was suggested many years ago by John Linsley [7]. But the use of the idea for charged particle detectors is problematic because of essential random fluctuations of the signal form. Figure 8 shows that in case of Cherenkov light random fluctuations do not play an essential role.

We realize that before using the second method of core reconstruction, the detailed study of WDF up to core distances 1000 – 1500 m has to be made not only with CORSIKA simulation but also experimentally. A positive result of this study would let us expand the sensitive area of the array for energies above $5 \cdot 10^{17}$ eV by 5 – 10 times compared with the geometrical area covered by the detectors.

Such sensitive area increase will provide 20-30 events with energies above 10^{18} eV during one year of observation and ensures an overlapping of the Tunka-133 energy range with that of huge installations such as Auger.

6. Unusual EAS longitudinal development

Among the events recorded by the first stage of the array a unique shower with very unusual waveforms of pulses at all the detectors was noticed. The core location for this shower determined by the traditional method of density light flux analysis was outside the array geometry. The experimental points of pulse waveform at one of detectors with EAS core distance ~700 m is shown in fig. 9. The waveform looks like containing two local maxima. The delay of the second maximum to the first one is about 150 ns. The waveforms of pulses at the other detectors are similar to this one but with slightly different delays between maxima.

The further analysis has shown the possibility of influence to the waveform of small clouds appearing at the sky at that time. The normal waveform coinciding with the observed one at the front and the tail of the pulse is shown by the curve in fig. 9. The observed waveform can be obtained from the normal one if to conceal a part of a shower track with a small cloud, because for the large core distance a different time in fig. 9 corresponds to a different direction in the sky.

Nevertheless the ability of the modern apparatus to record events with abnormal longitudinal development in the atmosphere is shown by this example. The main conclusion of this experience is that in order to search for events with unusual longitudinal development we have to introduce permanent monitoring of the optical conditions of the sky.

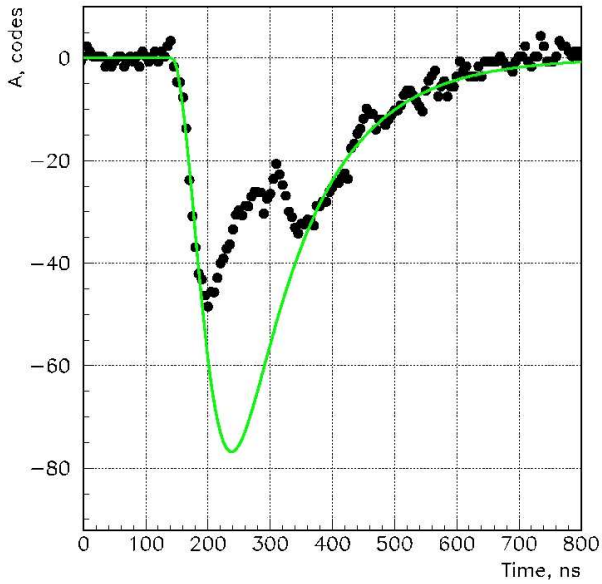

Figure 9. Abnormal experimental pulse waveform at a large core distance (~700 m). Curve – normal Cherenkov light pulse waveform.

Acknowledgments

This work is supported by Russian Federation Ministry of Science and Education (Contract No 02.518.11.7073), the Russian Foundation for Basic Research (grants 07-02-00904, 05-02-04010, 06-02-16526) and the German Research Foundation DFG(436 RUS 113/827/0-1).

References

[1] N. M. Budnev et al. "Cosmic Ray Energy Spectrum and Mass Composition from 10^{15} to 10^{17}eV by Data of the Tunka EAS Cherenkov Array," Proc. 29th ICRC. Pune, India, vol. 6, 2005 pp. 257-260.

[2] E. G. Berezhko, H. J. Volk "Spectrum of cosmic rays, produced in supernova remnants," 2007, arXiv:0704.1715.

[3] A. D. Panov et al. (ATIC Collaboration) "Energy spectra of primary cosmic ray separate nuclei by the data of the ATIC-2 experiment," Izv. RAS ser. phys., vol. 3, 2008 to be published.

[4] N. M. Budnev et al. "Tunka-133 EAS Cherenkov array: status of 2007," Proc. of 30th ICRC, Merida, Yucatan, Mexico, arXiv:0801.3037.

[5] E. E. Korosteleva et al. "Method of EAS Cerenkov light pulse shape measurement at the Tunka array," *Preprint of Scobeltsyn Institute of Nucl. Phys. MSU – 2004 – 2/740.*

[6] EAS-TOP Collaboration and Korosteleva E. E., Kuzmichev L. A., Prosin V. V. "Lateral distribution function of EAS Cherenkov light: experiment QUEST and CORSIKA simulation," Proc. 28th ICRC, Tsukuba, Japan, vol. 1, 2003, pp. 89-91.

[7] J. Linsley "Mini and super mini arrays for the study of highest energy cosmic rays**."** Proc. 19th ICRC. La Jolla. vol. 9, 1985, pp. 434-437.